Correction

BIOCHEMISTRY

Correction for "Fibulin-4 exerts a dual role in LTBP-4L–mediated matrix assembly and function," by Heena Kumra, Valentin Nelea, Hana Hakami, Amelie Pagliuzza, Jelena Djokic, Jiongci Xu, Hiromi Yanagisawa, and Dieter P. Reinhardt, which was first published September 23, 2019; 10.1073/pnas.1901048116 (*Proc. Natl. Acad. Sci. U.S.A.* **116**, 20428–20437).

The authors note that an additional affiliation should be listed for Hana Hakami. The new affiliation should appear as Faculty of Sciences and Medical Studies, College of Sciences, Zoology Department, King Saud University, Riyadh 12372, Saudi Arabia. The corrected author and affiliation lines appear below. The online version has been corrected.

The authors also note that the following statement should be added to the Acknowledgments: "H.H. received funding from the King Saud University and the Ottawa Cultural Bureau, Royal Embassy of Saudi Arabia."

Heena Kumra[a], Valentin Nelea[a,b], Hana Hakami[a,c], Amelie Pagliuzza[a], Jelena Djokic[a], Jiongci Xu[a], Hiromi Yanagisawa[d], and Dieter P. Reinhardt[a,b]

[a]Faculty of Medicine, Department of Anatomy and Cell Biology, McGill University, Montreal, QC H3A 0C7, Canada; [b]Faculty of Dentistry, McGill University, Montreal, QC H3A 0C7, Canada; [c]Faculty of Sciences and Medical Studies, College of Sciences, Zoology Department, King Saud University, Riyadh 12372, Saudi Arabia; and [d]Life Science Center of Tsukuba Advanced Research Alliance, University of Tsukuba, 305-8577 Tsukuba, Japan

First published December 16, 2019.

www.pnas.org/cgi/doi/10.1073/pnas.1920843117

Fibulin-4 exerts a dual role in LTBP-4L–mediated matrix assembly and function

Heena Kumra[a,1], Valentin Nelea[a,b,1], Hana Hakami[a,c], Amelie Pagliuzza[a], Jelena Djokic[a], Jiongci Xu[a], Hiromi Yanagisawa[d], and Dieter P. Reinhardt[a,b,2]

[a]Faculty of Medicine, Department of Anatomy and Cell Biology, McGill University, Montreal, QC H3A 0C7, Canada; [b]Faculty of Dentistry, McGill University, Montreal, QC H3A 0C7, Canada; [c]Faculty of Sciences and Medical Studies, College of Sciences, Zoology Department, King Saud University, Riyadh 12372, Saudi Arabia; and [d]Life Science Center of Tsukuba Advanced Research Alliance, University of Tsukuba, 305-8577 Tsukuba, Japan

Edited by Andrea Heinz, University of Copenhagen, Copenhagen, Denmark, and accepted by Editorial Board Member F. Ulrich Hartl August 30, 2019 (received for review January 23, 2019)

Elastogenesis is a hierarchical process by which cells form functional elastic fibers, providing elasticity and the ability to regulate growth factor bioavailability in tissues, including blood vessels, lung, and skin. This process requires accessory proteins, including fibulin-4 and -5, and latent TGF binding protein (LTBP)-4. Our data demonstrate mechanisms in elastogenesis, focusing on the interaction and functional interdependence between fibulin-4 and LTBP-4L and its impact on matrix deposition and function. We show that LTBP-4L is not secreted in the expected extended structure based on its domain composition, but instead adopts a compact conformation. Interaction with fibulin-4 surprisingly induced a conformational switch from the compact to an elongated LTBP-4L structure. This conversion was only induced by fibulin-4 multimers associated with increased avidity for LTBP-4L; fibulin-4 monomers were inactive. The fibulin-4–induced conformational change caused functional consequences in LTBP-4L in terms of binding to other elastogenic proteins, including fibronectin and fibrillin-1, and of LTBP-4L assembly. A transient exposure of LTBP-4L with fibulin-4 was sufficient to stably induce conformational and functional changes; a stable complex was not required. These data define fibulin-4 as a molecular extracellular chaperone for LTBP-4L. The altered LTBP-4L conformation also promoted elastogenesis, but only in the presence of fibulin-4, which is required to escort tropoelastin onto the extended LTBP-4L molecule. Altogether, this study provides a dual mechanism for fibulin-4 in 1) inducing a stable conformational and functional change in LTBP-4L, and 2) promoting deposition of tropoelastin onto the elongated LTBP-4L.

fibulin-4 | LTBP-4 | fibronectin | fibrillin-1 | elastic fibers

Elastogenesis is a highly hierarchical multistep molecular process by which cells form functional elastic fibers, providing elasticity to various soft tissues, including blood vessels, lung, and skin (1). This process begins with the secretion of fibronectin and its organization into a network, which acts as an organizer for the assembly of fibrillin-1 into microfibrils, as well as for the deposition of latent TGF-β binding protein (LTBP)-4, and fibulin-4 (2–6). The fibronectin network is not only required for the initiation of fibrillin-1 assembly, but is also essential for microfibril homoeostasis during early stages of matrix assembly (7). Tropoelastin, the soluble precursor of mature elastin, forms microaggregates on the cell surface, which are deposited onto microfibrils (8, 9). Elastic fiber formation requires several accessory proteins, including fibulin-4, fibulin-5, and LTBP-4 (10, 11). Fibulin-4 tethers lysyl oxidase and fibulin-5 lysyl oxidase like 1 to tropoelastin, facilitating cross-links required for the formation of nascent elastic fibers (12–14). LTBP-4S indirectly binds to tropoelastin via fibulin-5 and supports the linear deposition of fibulin-5, which in turn promotes elastic fiber formation (11). Here we report critical mechanistic roles of fibulin-4 and LTBP-4L in the hierarchical elastin assembly process.

Fibulin-4 and -5 are members of the fibulin family characterized by tandem repeats of calcium binding epidermal growth factor-like (cbEGF) domains and a C-terminal fibulin domain (1). Fibulin-4 multimerizes into a disk-shaped particle with an estimated 10 molecules (15). LTBP-4, a member of the LTBP family, shares structural homology with fibrillins, both characterized by extended cbEGF repeats interspersed with 8-cysteine (TB and hybrid) domains. Based on the domain composition and distribution, LTBP-4 is expected to adopt an extended structure, facilitating the linear deposition of tropoelastin onto microfibrils (11, 16–20). LTBP-4 exists in 2 major N-terminally distinct isoforms, the short (LTBP-4S) and the long (LTBP-4L), due to the usage of different promoters (21, 22). In humans, mutations in either fibulin-4, fibulin-5, or LTBP-4 result in autosomal recessive cutis laxa (ARCL) type 1B, 1A, and 1C, respectively, characterized by inelastic skin and pulmonary emphysema common to all types, and aortic tortuosity and aneurysm only caused by fibulin-4 mutations (23). A functional link has been established between LTBP-4L and fibulin-4 and between LTBP-4S and fibulin-5 using mouse models and cell culture studies (11, 20, 24). Fibulin-4 depends on LTBP-4L for its assembly/deposition (25). A reduced interaction of LTBP-4L with fibulin-4 in $Ltbp4S^{-/-}$; $Fbln4^{R/R}$ mice results in impaired elastogenesis (24). However, elastogenesis in $Ltbp4S^{-/-}$; $Fbln5^{-/-}$ double-knockout mice was improved as compared to $Ltbp4S^{-/-}$ mice (20). Despite some known functional relationships between the elastogenic proteins, the underlying molecular mechanisms that drive hierarchical elastin assembly are largely elusive.

Significance

Soft tissues such as blood vessels, lung, and skin require various extracellular proteins, including tropoelastin, fibrillins, fibulin-4, and latent TGF-β binding protein-4 (LTBP-4) to synthesize functional elastic fibers in a highly hierarchical fashion. Mutations in these proteins cause heritable diseases, resulting in deficient elastic fibers and function. We provide evidence for a dual role of fibulin-4 in this context. Our results demonstrate how physical interactions between these elastogenic proteins play key roles in inducing conformational and functional changes, which then impacts self-assembly and elastic fiber formation. This fundamental finding is essential to understand the pathogenesis of diseases associated with mutations in elastogenic proteins.

Author contributions: H.K., V.N., and D.P.R. designed research; H.K., V.N., H.H., A.P., J.D., and J.X. performed research; H.H. and H.Y. contributed new reagents/analytic tools; H.K., V.N., and D.P.R. analyzed data; and H.K., V.N., and D.P.R. wrote the paper.

The authors declare no conflict of interest.

This article is a PNAS Direct Submission. A.H. is a guest editor invited by the Editorial Board.

[1]H.K. and V.N. contributed equally to this work.

[2]To whom correspondence may be addressed. Email: dieter.reinhardt@mcgill.ca.

This article contains supporting information online at https://www.pnas.org/lookup/suppl/doi:10.1073/pnas.1901048116/-/DCSupplemental.

First published September 23, 2019.

In this study we analyze the molecular interaction between fibulin-4 and LTBP-4L and its structural consequence. We determine the functional relationship of fibulin-4 and LTBP-4L with the central elastogenic proteins fibronectin, fibrillin-1, and tropoelastin and define the significance of these interactions on matrix assembly and function. Employing a series of biophysical, cell culture, and in vivo approaches, we show that fibulin-4 has a dual role in respect to LTBP-4L, first triggering structural changes and functional activation of LTBP-4L, and then transporting tropoelastin onto fibrillin-supported elongated LTBP-4L assemblies.

Results

Fibulin-4 Multimerizes via Interactions of Central and C-Terminal Domains. We have previously discovered that fibulin-4 has the propensity to self-oligomerize under physiological conditions, giving rise to multimers (15). Here, we explore how fibulin-4 multimers form, and define the functional significance of this property on fibulin-4 interactions with other elastogenic proteins. To determine which region of fibulin-4 is involved in self-interaction, 3 nonoverlapping recombinant fibulin-4 fragments were generated: 1) Nterm-cbEGF1 comprising the N-terminal domain and the first cbEGF domain (~10.8 kDa); 2) cbEGF2-5 encompassing cbEGF domains 2 to 5 (~18.6 kDa); and 3) cbEGF6-Cterm including the sixth cbEGF domain and the C-terminal fibulin unique region (~18.3 kDa) (Fig. 1*A*). Dynamic light scattering (DLS) (Fig. 1*B*) showed for the Nterm-cbEGF1 fragment a single monodisperse population of particles with a hydrodynamic radius (R_h) of 2.5 nm. The central fragment cbEGF2-5 displayed a dominant monodisperse population of particles with much larger sizes (R_h = 17.4 nm). Similarly, the cbEGF6-Cterm fragment showed a dominant monodisperse population of R_h = 16.8 nm. These data indicate that the central and C-terminal fibulin-4 fragments can multimerize, since for monomeric populations of these fragments the hydrodynamic radii are predicted to be below 3 nm. Additionally, SDS/PAGE analysis demonstrated for these fibulin-4 fragments protein bands with molecular masses attributable to multimers under nonreducing conditions and monomers under reducing conditions (Fig. 1 *A*, *Right*, arrow), whereas Nterm-cbEGF1 was monomeric under both conditions. In summary, these data demonstrate the presence of at least 2 multimerization sites in fibulin-4, 1 in the center and 1 in the C-terminal region.

The fibulin-4 fragments were then analyzed by surface plasmon resonance (SPR) to determine self-interaction with full-length fibulin-4 (Fig. 1*C*). The Nterm-cbEGF1 bound negligibly to fibulin-4 (K_D = 1,137 ± 240 nM), confirming that the N terminus has no role in multimerization. However, the fragments cbEGF2-5 and cbEGF6-Cterm exhibited appreciable binding to fibulin-4 with affinities of K_D = 104 ± 16 nM and K_D = 74 ± 13 nM, respectively, which is in the similar range determined for the full-length fibulin-4 self-interaction (K_D = 85 ± 15 nM) (*SI Appendix*, Fig. S1), demonstrating that fibulin-4 multimerizes by interactions of central and C-terminal domains. To determine to what extent multimerization of fibulin-4 affects its self-interaction property, full-length fibulin-4 was first separated by gel-filtration into monomers, dimers, and multimers, as previously shown (15), and then used in SPR to determine their binding affinities to nongel-filtrated fibulin-4. The monomers did not bind to fibulin-4, dimers bound with residual weak affinity, and multimers showed strong binding to fibulin-4 [K_D = 2.7 ± 1.1 nM; calculated using the estimate of 10 monomers per multimer (15)] (Fig. 1*D*). These data clearly demonstrated that fibulin-4 increases its avidity for self-interaction upon multimerization.

Fibulin-4 Assembly Is Directly Dependent on Fibronectin and Is Not Mediated via Fibrillin-1. Recently, we have shown in mouse models and cell culture that fibulin-4 assembly/deposition is abolished upon loss of fibronectin (6). However, it is not clear whether this represents the loss of a potentially direct fibulin-4–fibronectin interaction, or the loss of fibulin-4 interaction with fibrillin-1 (26), which requires fibronectin for its assembly (2, 3). Here, we determined by SPR that fibulin-4 can indeed directly interact with fibronectin with a K_D = 177 ± 48 nM (Fig. 2*A*). The 2 proteins also completely colocalized in the extracellular matrix produced by dermal fibroblasts (Fig. 2*B*). Fibronectin interaction sites on fibulin-4 were mapped to the central (cbEGF2-5; K_D = 12.6 ± 2.1 nM) and the C-terminal (cbEGF6-Cterm; K_D = 13.5 ± 2.7 nM) regions of fibulin-4 (Fig. 2*C*). We further examined the contribution of fibulin-4 monomers, dimers, and multimers in fibronectin interaction. SPR experiments demonstrated that only the multimers efficiently interacted with fibronectin (K_D = 16.2 ± 4.5 nM), but not the monomers and the dimers, suggesting that multimerization of fibulin-4 promotes fibronectin binding (Fig. 2*D*).

In addition to the interaction with fibronectin, fibulin-4 also binds to fibrillin-1 (5, 12, 26). Determining the binding sites and affinities revealed a different interaction pattern of fibulin-4 to fibrillin-1 as compared to fibronectin. Nterm-cbEGF1 bound the strongest to fibrillin-1 (K_D = 3.2 ± 0.6 nM) followed by the central cbEGF2-5 fragment (K_D = 14.4 ± 3.5 nM), whereas cbEGF6-Cterm showed no binding (Fig. 2*E*). Fibulin-4 showed higher binding affinity to fibrillin-1 compared to fibronectin [K_D = 7.9 ± 1.5 nM for fibrillin-1 (Fig. 2*E*) vs. K_D = 177 ± 48 nM for fibronectin (Fig. 2*A*)]. Fibulin-4 colocalized with fibrillin-1,

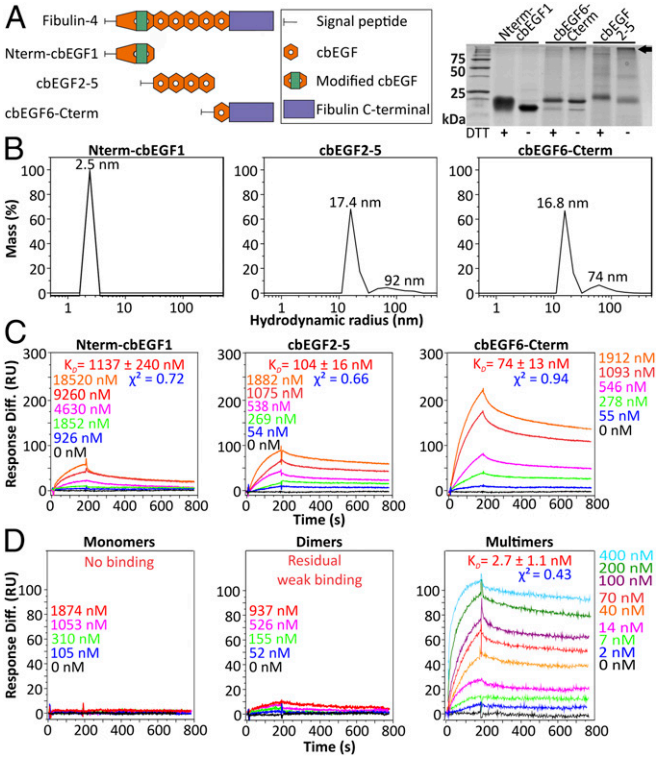

Fig. 1. Fibulin-4 self-interacts via a central and a C-terminal region. (*A*) Schematic diagram of full-length fibulin-4 and the consecutive nonoverlapping Nterm-cbEGF1, cbEGF2-5, and cbEGF6-Cterm fragments (*Left*). SDS/PAGE of fibulin-4 fragments under reducing (+) and nonreducing (–) conditions (*Right*). The arrow points to high molecular mass species of cbEGF2-5 and cbEGF6-Cterm. (*B*) Mass size distributions of Nterm-cbEGF1, cbEGF2-5, and cbEGF6-Cterm determined by DLS. The *x* axis shows the particle hydrodynamic radius of the protein sample on a logarithmic scale, and the *y* axis the mass percentages of particles of a given hydrodynamic radius present in the sample. The peaks represent particle populations with radius sizes indicated on top. Note that the higher molecular mass protein bands in the SDS/PAGE for cbEGF6-Cterm and cbEGF2-5 (*A*, *Right*) correlate with peaks corresponding to larger sizes in DLS (*B*). (*C* and *D*) SPR sensorgrams of the interaction of the fibulin-4 fragments Nterm-cbEGF1, cbEGF2-5, and cbEGF6-Cterm (*C*), and of gel-filtrated full-length fibulin-4 monomers, dimers, and multimers (*D*) with full-length nongel-filtrated fibulin-4 immobilized on the chip. Note the binding of cbEGF2-5 and cbEGF6-Cterm in *C* and the particularly strong binding of multimers in *D*.

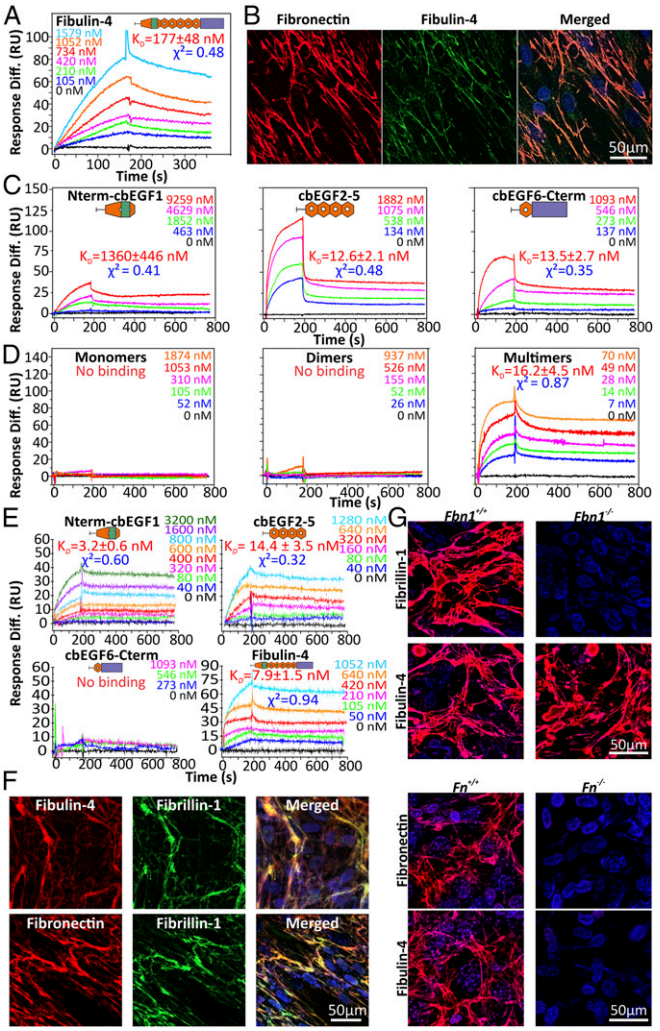

Fig. 2. Fibulin-4 interacts with and assembles on fibronectin. (*A*) SPR sensorgram of the interaction of fibronectin (immobilized) with fibulin-4 (soluble). (*B*) Colocalization of fibronectin (red) with fibulin-4 (green) in the extracellular matrix produced by human skin fibroblasts 6 d after cell seeding, evident in the merged image (yellow). (*C* and *D*) SPR sensorgrams of the interaction of fibronectin (immobilized) with the soluble fibulin-4 fragments Nterm-cbEGF1, cbEGF2-5 and cbEGF6-Cterm (*C*), and with gel-filtrated full-length soluble fibulin-4 monomers, dimers, and multimers (*D*). Note that the binding sites for fibronectin are in the central and C-terminal region of fibulin-4, and that binding only occurs with multimers. (*E*) SPR sensorgrams of soluble Nterm-cbEGF1, cbEGF2-5, cbEGF6-Cterm, and full-length fibulin-4 as a control with the N-terminal half of fibrillin-1 (immobilized). Binding sites are located in the N-terminal cbEGF domain and the central region of fibulin-4. (*F*, *Upper*) Colocalization of fibulin-4 (red) with fibrillin-1 (green) in the matrix produced by human skin fibroblasts 6 d after cell seeding. (*Lower*) Fibrillin-1 (green) colocalizes with fibronectin (red) under identical conditions. (*G*) Immunofluorescence of fibulin-4 in the extracellular matrix of mouse skin fibroblasts either lacking *Fbn-1* (*Upper*) or *Fn* (*Lower*) after addition of exogenous fibulin-4. Before analyzing the cells, 25 μg/mL purified fibulin-4 was added for 1 d. Note the absence of fibrillin-1 assembly in $Fbn1^{-/-}$ cells whereas fibulin-4 assembly was normal and comparable to $Fbn1^{+/+}$ control cells. Both, fibronectin and fibulin-4 assembly was not detectable in the matrix produced by $Fn^{-/-}$ cells.

which in turn colocalized to fibronectin in the matrix produced by human skin fibroblasts (Fig. 2*F*) (3). To understand whether fibulin-4 assembly/deposition is dependent on fibronectin or on fibrillin-1, we employed knockout skin fibroblasts. The addition of exogenous fibulin-4 to $Fbn1^{-/-}$ mouse skin fibroblasts resulted in a similar fibulin-4 assembly/deposition as compared to the $Fbn1^{+/+}$ control cells (Fig. 2 *G*, *Upper*), demonstrating that fibulin-4 can assemble/deposit in the matrix in the absence of fibrillin-1. However, the absence of fibronectin abolished fibulin-4 assembly/deposition, clarifying a direct dependency of fibulin-4 assembly/deposition on fibronectin (Fig. 2 *G*, *Lower*).

LTBP-4L Undergoes a Conformational Change upon Interaction with Fibulin-4. Fibulin-4 assembly also depends on LTBP-4L, and the 2 proteins interact with each other (24, 25). Mapping of the interaction sites by SPR revealed the center of fibulin-4 as the strongest binding site for LTBP-4L (K_D = 15.3 ± 3.7 nM) and a minor binding site located at the fibulin-4 C terminus (K_D = 260 ± 14 nM) (Fig. 3*A*). To determine potential structural consequences of this interaction, we analyzed LTBP-4L either alone or in the presence of fibulin-4 (nongel-filtrated) by atomic force microscopy (AFM) (Fig. 3*B* and Table 1). Surprisingly, only a relatively small portion of the LTBP-4L molecules (35%) adopted the expected extended conformation (based on the cbEGF and TB-rich domain composition) in the absence of fibulin-4. Most LTBP-4L molecules (65%) showed a compact or semicompact conformation (Fig. 3 *B*, *Left*). However, after the addition of an excess of fibulin-4 (LTBP-4L:fibulin-4 molar ratio of 1:10), almost twice as many LTBP-4L molecules (68%) adopted an extended conformation with an average length of 78 nm, correlating well with the expected length based on the number of tandem cbEGF domains interspersed with TB domains (27–29) (Fig. 3 *B*, *Center*, and Table 1). The molar excess of fibulin-4 was required as an equimolar 1:1 LTBP-4L:fibulin-4 ratio, or a 10-fold molar excess of LTBP-4L was not effective in changing the LTBP-4L structure (*SI Appendix*, Fig. S2*A*). It can be assumed that the extended molecules do not represent fibulin-4 molecules as they adopt disk-shaped particles (15). In some instances, filamentous structures much longer than 78 nm were observed. Since LTBP-4L has self-interaction capabilities (*SI Appendix*, Fig. S2*B*), those long filaments are very likely self-assemblies of LTBP-4L molecules. Addition of EDTA to the LTBP-4L/fibulin-4 mixture reverts almost entirely (94%) the extended conformation to the compact structure of LTBP-4L (Fig. 3 *B*, *Right*, and Table 1), suggesting the requirement of Ca^{2+} for stabilization of the LTBP-4L extension.

To further validate this fibulin-4–driven extension of LTBP-4L, we analyzed the LTBP-4L/fibulin-4 mixture by DLS. The particle sizes of the mixture were larger than those of LTBP-4L alone or fibulin-4 alone, with hydrodynamic radii of 11.2 nm for the mixture versus 8.4 nm for LTBP-4L or 3.6 nm for fibulin-4 (Fig. 3*C*), further supporting a conformational change by extension of LTBP-4L upon interaction with fibulin-4. Next, we analyzed whether the interaction with and the conformational change induced in LTBP-4L is dependent on the multimerization of fibulin-4. SPR revealed that it is the fibulin-4 multimers that bind to LTBP-4L (K_D = 2.2 ± 1.0 nM), but not lower molecular mass species (Fig. 3*D*). To analyze the consequence of fibulin-4 multimerization on the induction of the conformational change in LTBP-4L, we mixed gel-filtrated fibulin-4 monomers, dimers, or multimers with LTBP-4L (LTBP-4L:fibulin-4 monomer ratio of 1:10) and performed AFM analyses. The extension of LTBP-4L was primarily induced by fibulin-4 multimers (constituted by ∼10 molecules), but not by monomers or dimers (Fig. 3*E* and Table 1), demonstrating that fibulin-4 multimerization is essential to induce the conformational changes in LTBP-4L. In summary, these data demonstrate that the interaction of fibulin-4 multimers with LTBP-4L induces an unexpected extension of LTBP-4L, switching its shape from a closed conformation to a primarily open elongated structure.

The Conformational Change in LTBP-4L Modifies Its Function. To explore whether the fibulin-4–induced conformational change in LTBP-4L impacts its functionality, we tested its binding to key elastogenic proteins, fibrillin-1 and fibronectin. Interestingly, in the presence of fibulin-4, LTBP-4L displayed enhanced binding to fibrillin-1 in solid-phase binding assays (Fig. 4*A*), whereas it reduced

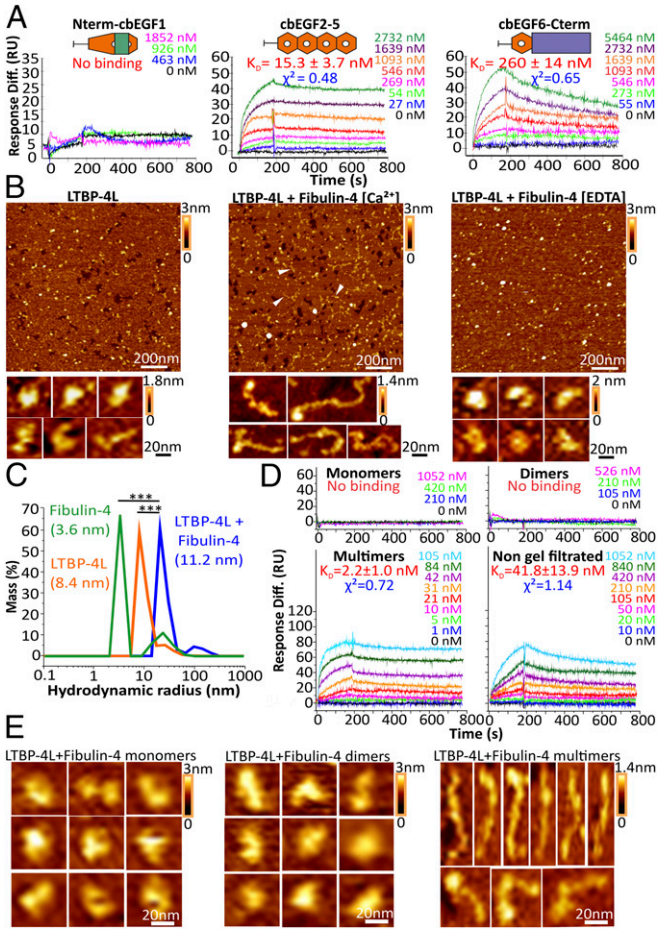

Fig. 3. Conformational change in LTBP-4L induced by fibulin-4 multimers. (*A*) SPR sensorgrams of the interaction of Nterm-cbEGF1, cbEGF2-5 and cbEGF6-Cterm with immobilized LTBP-4L. (*B*) AFM height images showing LTBP-4L alone (*Left*), a 1:10 molar ratio of a LTBP-4L/fibulin-4 mixture in the presence of $CaCl_2$ (*Center*), or 10 mM EDTA (*Right*) with higher magnification views of representative conformations of individual particles (*Lower*). Arrowheads indicate some elongated particles. (*C*) DLS mass size distribution of fibulin-4 alone, LTBP-4L alone, and a 1:10 molar ratio of a LTBP-4L/fibulin-4 mixture. The particle hydrodynamic radius is plotted logarithmically on the *x* axis and the mass percentages of particles on the *y* axis. Note the significant change in hydrodynamic radius upon mixing LTBP-4L with fibulin-4 as compared to fibulin-4 alone or LTBP-4L alone. ***$P < 0.0001$ (2-sample *t* test). (*D*) SPR sensorgrams of immobilized LTBP-4L with gel-filtrated full-length fibulin-4 monomers, dimers, multimers, and nongel-filtrated fibulin-4. Note that only fibulin-4 multimers and nongel-filtrated fibulin-4 (which contains multimers) interact with LTBP-4L. (*E*) AFM height images showing representative particles of mixtures of LTBP-4L with fibulin-4 monomers, dimers, and multimers at a 1:10 molar ratio (LTBP-4L:fibulin-4 monomer unit).

the binding to fibronectin (Fig. 4*B*), compared to LTBP-4L alone. Functional consequences of the fibulin-4–induced conformational change in LTBP-4L were further tested on LTBP-4L assembly in cell culture. Purified LTBP-4L, fibulin-4, or a mixture of LTBP-4L and fibulin-4 (1:10 molar ratio) was added to human skin fibroblasts (Fig. 4*C*). Addition of either LTBP-4L or fibulin-4 alone did not change the assembly of LTBP-4 as compared to the buffer control, indicating that neither LTBP-4L nor fibulin-4 alone can promote LTBP-4 assembly. However, addition of the LTBP-4L/fibulin-4 mixture promoted LTBP-4 assembly, suggesting that it is the fibulin-4–induced extended conformation of LTBP-4L that promotes fibrous self-assembly. This result correlates with the data presented in Fig. 3*B*, showing extended LTBP-4L filamentous structures only developed in the presence of fibulin-4. If fibulin-4 indeed plays a role in LTBP-4 assembly, then the complete absence of fibulin-4 should affect the assembly/deposition of LTBP-4 in vivo. This hypothesis was confirmed with aortic tissues from wild-type and from global fibulin-4 knockout mice (30). Immunostaining of LTBP-4 in these aortic sections showed a significantly lower amount (65%) of LTBP-4 in the fibulin-4 knockout tissues as compared to wild-type controls (Fig. 4 *D* and *E*). Overall, these data demonstrate that the fibulin-4–induced conformational change in LTBP-4L modulates interaction with fibrillin-1 and fibronectin, and promotes LTBP-4L filamentous self-assembly.

Fibulin-4 Acts as a Chaperone That Mediates a Stable LTBP-4L Conformational Change. We analyzed the time course of the LTBP-4L conformational change after exposure to fibulin-4 at a 1:10 molar ratio using AFM and DLS (Fig. 5). AFM analysis showed that the LTBP-4L extended conformation was stable over time (up to 48 h, the maximum analyzed time) (Fig. 5*A*). Real-time DLS mass distribution showed that the conformational change of LTBP-4L completed within 20 min after mixing with fibulin-4, with an increase of R_h from 9.3 nm at 0 min to 12.1 nm at 20 min (Fig. 5*B*, boxed area, and Fig. 5*C*). As in the AFM analysis, the extended conformation was stable for the remaining analysis time up to 300 min (Fig. 5*B*, black symbols). Approximately every 45 to 70 min, the R_h of the fibulin-4/LTBP-4L complex (11 to 12 nm) changed to a larger R_h, ranging from 11.3 to 25.5 nm, and simultaneously a second smaller R_h between 3.6 and 5.1 nm (Fig. 5*B*, red and blue symbols, and Fig. 5*C*). This split in mass distribution periodically reverted back after approximately 20 to 35 min, consistently resulting in particles with R_h values similar to that of a complex between fibulin-4 and the extended LTBP-4L monomer (R_h = 11 to 12 nm) (Fig. 5 *B* and *C*). This suggests that fibulin-4 periodically dissociated from the extended LTBP-4L, which allowed noncovalent multimerization of LTBP-4L into oligomers. However, since fibulin-4 remained in the in vitro system, it continued to compete with LTBP-4L oligomerization, reversibly resulting in complex formation between the 2 proteins.

To further validate if the fibulin-4–induced conformational change in LTBP-4L persists in the absence of fibulin-4, we first passed LTBP-4L over a covalently bound fibulin-4 chromatography resin during an extended time to allow binding and dissociation of LTBP-4L (FBLN-4 primed LTBP-4L) (*SI Appendix*, Fig. S3*A*). Extensive characterization of the fibulin-4–primed LTBP-4L by ELISA and by Western blot clearly demonstrated the complete absence of fibulin-4 in the dissociated fraction eluted from the column and validated the presence of LTBP-4L (*SI Appendix*, Fig. S3 *B* and *C*). AFM imaging of the fibulin-4–primed LTBP-4L predominately showed elongated molecules of 81 nm in length, similar to the length of LTBP-4L determined in the mixture with fibulin-4 (78 nm) (Fig. 6*A* and Table 1). Correlating with these data, DLS analysis showed larger particle sizes for the fibulin-4–primed LTBP-4L (R_h = 11.8 nm) compared to LTBP-4L that was not exposed to fibulin-4 (R_h = 8.4 nm), very similar to that obtained with a mixture of LTBP-4L and fibulin-4 (R_h = 11.2 nm) (Fig. 6*B*). Altogether, these data demonstrate that the fibulin-4–induced conformational change of LTBP-4L persisted even in the absence of fibulin-4, suggesting that fibulin-4 acts as a chaperone for LTBP-4L.

We then addressed if the functional change observed in the mixture of LTBP-4L with fibulin-4 in regard to interacting ligands and self-assembly can be reproduced with the fibulin-4–primed LTBP-4L. We conducted SPR experiments of fibulin-4–primed LTBP-4L or LTBP-4L alone (not exposed to fibulin-4) in liquid phase with immobilized fibrillin-1 (N-terminal half) (Fig. 6*C*) or fibronectin (Fig. 6*D*). Consistent with the results for the mixture of fibulin-4 with LTBP-4L obtained with solid-phase binding assays, fibulin-4–primed LTBP-4L showed enhanced binding to the fibrillin-1 N-terminal half (K_D = 0.45 ± 0.12 nM versus K_D = 12.3 ± 1.8 nM for LTBP-4L nonprimed), and reduced binding to fibronectin (K_D = 8.2 ± 2.5 nM versus K_D = 2.1 ± 0.9 nM for LTBP-4L nonprimed). We then analyzed the ability of the extended LTBP-4L to interact with fibulin-4, which was not possible

Table 1. Quantification of structural LTBP-4 classes

Feature molecules	Compact diameter, nm	Extended length, nm	Compact no., %	Semicompact no., %	Extended no., %
LTBP-4L	25 ± 5	61 ± 7	25 ± 9	40 ± 12	35 ± 6
LTBP-4L + fibulin-4	31 ± 16	78 ± 16*	18 ± 7	14 ± 6	68 ± 11*
LTBP-4L + fibulin-4 multimers	28 ± 10	80 ± 14*	17 ± 5	12 ± 6	71 ± 14*
Fibulin-4 primed LTBP-4L	38 ± 7	81 ± 12*,†	16 ± 4	11 ± 4	73 ± 15*
LTBP-4L + fibulin-4 [EDTA treated]	34 ± 18	ND	94 ± 1	4 ± 0.5	2 ± 0.3*,†
LTBP-4L + fibulin-5	27 ± 5	69 ± 11*,†	24 ± 8	25 ± 5	51 ± 8*,†
LTBP-4S	29 ± 12	ND	86 ± 2	11 ± 1	3 ± 0.5
LTBP-4S + fibulin-4	34 ± 16	ND	89 ± 8	9 ± 2	2 ± 0.8

The data represents from top to bottom quantification of LTBP-4L alone (Fig. 3*B*), in a mixture with nongel-filtrated fibulin-4 (Fig. 3*B*), in a mixture with fibulin-4 multimers (Fig. 3*E*), primed with fibulin-4 (Fig. 6*B*), in a EDTA-treated mixture with nongel filtrated fibulin-4 (Fig. 3*B*), or in a mixture with fibulin-5 (nongel-filtrated) (Fig. 7*B*), and of LTBP-4S alone or in a mixture with fibulin-4 (*SI Appendix*, Fig. S6). ND, not determined.
*Denotes a significant difference ($P < 0.01$) as compared to LTBP-4L.
†Denotes a significant difference ($P < 0.01$) as compared to LTBP-4L + nongel filtrated fibulin-4.

when fibulin-4 was present in the mixture. This resulted in an enhanced affinity of the fibulin-4–primed LTBP-4L to fibulin-4 (K_D = 22.2 ± 5.1 nM versus K_D = 44.7 ± 6.2 nM for LTBP-4L nonprimed) (Fig. 6*E*). SPR analysis showed negligible binding of fibulin-4–primed LTBP-4L to tropoelastin, similar to published data (*SI Appendix*, Fig. S4) (11). Analysis of self-interaction properties showed higher binding affinity for the fibulin-4–primed LTBP-4L (K_D = 5.5 ± 0.8 nM versus K_D = 47.2 ± 12.5 nM for LTBP-4L nonprimed) (Fig. 6*F*). To assess the significance of the enhanced LTBP-4L self-interaction in cell culture, fibulin-4–primed LTBP-4L was added to human skin fibroblasts and analyzed by immunofluorescence. The fibulin-4–primed LTBP-4L assembled in a similar manner than the mixture of LTBP-4L and fibulin-4 (Fig. 6 *G* and *H*). These data show that a transient interaction of LTBP-4L with fibulin-4 is sufficient to induce a stable conformational and consequently functional changes in LTBP-4L that modulate protein–ligand interaction and self-assembly.

Fibulin-4 Tethers Tropoelastin onto Extended LTBP-4L Structures. Next, we analyzed whether and how the fibulin-4–induced conformational change of LTBP-4L has consequences on tropoelastin multimerization. First, we added purified tropoelastin either to a LTBP-4L/fibulin-4 mixture (1:10 molar ratio) or to fibulin-4–primed LTBP-4L and performed AFM analyses. Only the LTBP-4L/fibulin-4 mixture mediated large and extended tropoelastin assemblies, whereas either fibulin-4–primed LTBP-4L or the individual proteins alone did not promote such large tropoelastin assemblies (Fig. 7*A*). This result was further corroborated by DLS experiments, which showed a shift to a much larger hydrodynamic radius and thus particle sizes upon mixing LTBP-4L/fibulin-4 with tropoelastin. This was not observed for the other protein combinations tested (Fibulin-4/tropoelastin, LTBP-4L/tropoelastin, Fibulin-4–primed LTBP-4L/tropoelastin) (Fig. 7*B*). These results suggested the requirement of all 3 proteins (LTBP-4L, fibulin-4, and tropoelastin) for the formation of tropoelastin multimers. These data were further validated in cell culture with human skin fibroblasts. Addition of a LTBP-4L/fibulin-4 mixture to the fibroblast culture medium resulted in long mature elastin fibers (Fig. 7*C*, white arrowheads). However, the addition of either fibulin-4–primed LTBP-4L or LTBP-4L alone did not promote assembly of extended elastin fibers, with tropoelastin deposits on cells remaining small and punctuated. Addition of fibulin-4 alone resulted only in a few short very thin elastin fibers (Fig. 7*C*, red arrowheads), confirming that both the extended LTBP-4L and fibulin-4 are essential for the formation of mature elastin fibers. This prompted us to determine the binding site and affinity of fibulin-4 for the tropoelastin/fibulin-4 interaction. SPR experiments using the recombinant fibulin-4 fragments in the soluble phase and immobilized tropoelastin demonstrated that the central cbEGF2-5 fragment interacted with K_D = 28.8 ± 14.0 nM and the C-terminal cbEGF6-Cterm fragment with a K_D = 30.8 ± 11.1 nM, both very similar to the binding of full-length fibulin-4 to tropoelastin (K_D = 21.8 ± 12.3 nM) (Fig. 7*D*). Overall, these results show that fibulin-4 is required for the deposition of elastin on elongated LTBP-4L fibers.

Fibulin-5 Induces the LTBP-4L Conformational Change Similar to Fibulin-4 but without the Functional Consequences. Since fibulin-5 also binds LTBP-4L (25), we analyzed whether fibulin-5 can induce

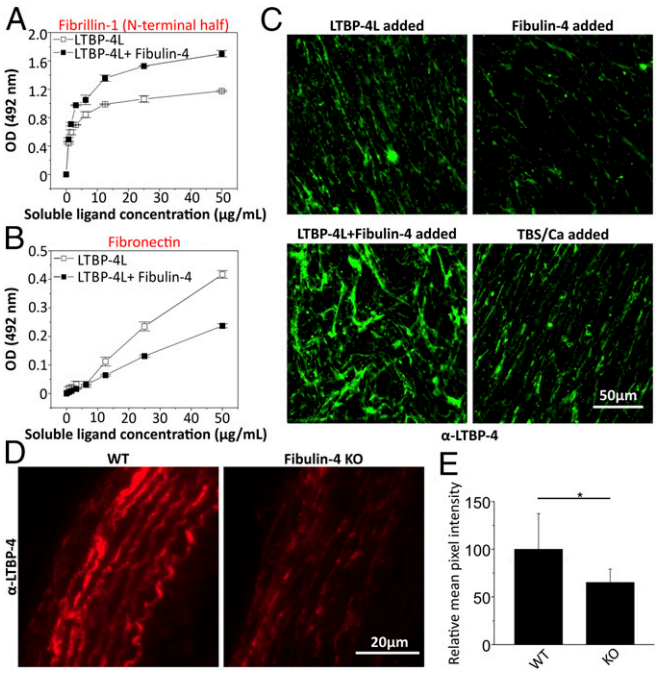

Fig. 4. Functional change in LTBP-4L induced by fibulin-4. (*A* and *B*) Solid-phase binding assays of LTBP-4L and 1:10 molar ratio LTBP-4L/fibulin-4 mixture used as soluble ligand on coated fibrillin-1 N-terminal half (*A*) and fibronectin (*B*). A specific antiserum was used for detection of bound LTBP-4. Note that the LTBP-4L/fibulin-4 mixture (closed symbols) mediates a stronger binding to fibrillin-1 (*A*) and a reduced binding to fibronectin (*B*) as compared to LTBP-4L alone (open symbols). (*C*) Effect of fibulin-4–induced conformational change of LTBP-4L on LTBP-4 assembly in cell culture. For this, 10 μg/mL of LTBP-4L alone or 27 μg/mL of fibulin-4 alone or a mixture of 10 μg/mL of LTBP-4L and 27 μg/mL of fibulin-4 (molar ratio of 1:10) was added to human skin fibroblasts for 7 d prior to immunofluorescence analysis. TBS/2 mM $CaCl_2$ was used as buffer control. Note the enhanced LTBP-4 assembly upon addition of the LTBP-4L/fibulin-4 mixture as compared to addition of the individual proteins. (*D*) LTBP-4 staining in wild-type (WT) and fibulin-4 knockout (KO) aorta harvested at embryonic day 17.5. (*E*) Quantification of the staining in (*D*). *$P < 0.05$ (2-sample *t* test). Note the reduced LTBP-4 staining, indicating reduced assembly/deposition in the absence of fibulin-4.

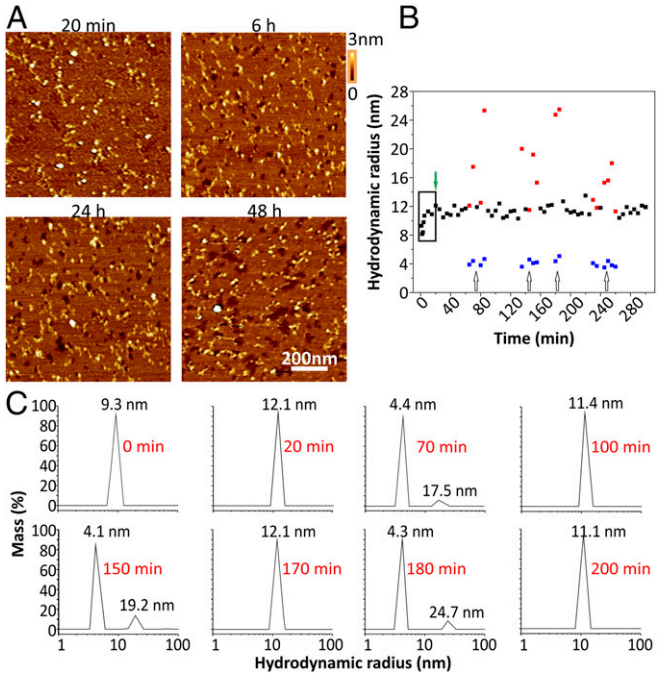

Fig. 5. Dynamics of fibulin-4 induced conformational change in LTBP-4L. (*A*) AFM height images showing a time course analysis of a LTBP-4L/fibulin-4 mixture (1:10 molar ratio) at endpoints 20 min, 6 h, 24 h, and 48 h after mixing. Note that the fibulin-4–induced conformational change of LTBP-4L, which is observed as early as 20 min (also evident from Fig. 3*B*), did not reverse within the analysis time. (*B*) Real-time DLS mass distribution analysis of a LTBP-4L/fibulin-4 mixture (1:10 molar ratio) within 0 to 300 min. Black symbols represent data points where a single peak was observed, red and blue symbols represent the larger and smaller size data points, respectively, when 2 peaks appeared. At each time point there was either 1 single peak (black symbol) or 2 peaks (red and blue symbol), but never 3 peaks. The boxed area highlights the time span in which extension of LTBP-4L becomes fully induced. The green arrow points to a 20-min time point after which the extension was stable. The white arrows show a periodic pattern of dissociation. (*C*) Selected mass distribution plots obtained from the real-time DLS analysis (plotted in *B*), demonstrating events of association and conformational changes between LTBP-4L and fibulin-4 (0 to 20 min), and events of periodic dissociation and association between the extended LTBP-4L and fibulin-4. The *x* axis shows on a logarithmic scale the particle hydrodynamic radius of the protein sample in nanometers, and the *y* axis represents the mass percentages of particles with a given hydrodynamic radius in the sample.

the LTBP-4L extended conformation. SPR experiments confirmed the fibulin-5/LTBP-4L interaction (K_D = 45.2 ± 8.4 nM) (*SI Appendix*, Fig. S5*A*). To assess if LTBP-4L undergoes a conformational change upon interaction with fibulin-5, LTBP-4L was mixed with fibulin-5 under identical conditions used previously for fibulin-4 (1:10 molar ratio LTBP4L:fibulin-5). While many LTBP-4L molecules appeared elongated in AFM (Fig. 7*E*), quantification showed a significantly lower percentage (51%) of extended LTBP-4L particles compared to the presence of fibulin-4 in this assay (68%) (Table 1). Additionally, the mean length of fibulin-5–induced LTBP-4L was significantly shorter (69 nm) than that of the fibulin-4–induced LTBP-4L (78 nm) (Table 1). Next, we investigated if the fibulin-5–induced partial extension of LTBP-4L has similar functional consequences as the fibulin-4–induced LTBP-4L. Solid-phase binding assays of soluble LTBP-4L alone and LTBP-4L/fibulin-5 mixtures (1:10 molar ratio) showed no difference in LTBP-4L binding to fibrillin-1 or fibronectin (*SI Appendix*, Fig. S5 *B* and *C*). These data demonstrate that the conformational change in LTBP-4L induced by fibulin-5, unlike fibulin-4, is not sufficient to affect the binding interaction with fibrillin-1 and fibronectin. Finally, we assessed the consequences of the fibulin-5–driven LTBP-4L extension in tropoelastin deposition under identical experimental conditions than used for fibulin-4 (Fig. 7*E*). When LTBP-4L, fibulin-5, and tropoelastin were mixed together, short extended and branched structures were observed. This aggregation pattern differed from the patterns identified in the presence of fibulin-4, which showed more unidirectional and longer structures (compare Fig. 7*E* with Fig. 7 *A*, *Left*). These data suggest different roles for fibulin-4 and -5 in driving the organization of tropoelastin onto the elongated LTBP-4L arrays.

The Short LTBP-4S Isoform Does Not Undergo a Conformational Change upon Interaction with Fibulin-4. LTBP-4 exists in 2 isoforms, the long (LTBP-4L) and the N-terminally truncated form (LTBP-4S). Recombinant LTBP-4S adopted a similar compact shape as LTBP-4L (*SI Appendix*, Fig. S6 *A*, *Left*). As shown previously (25), fibulin-4 did interact with LTBP-4S (K_D = 370 ± 48 nM), albeit with about a 10-fold lower affinity than the interaction between LTBP-4L and fibulin-4 (compare *SI Appendix*, Fig. S6*B* with Fig. 3*D*, nongel-filtrated). To analyze whether the interaction of LTBP-4S with fibulin-4 facilitated an extended structure, we performed AFM with LTBP-4S alone or in a mixture with fibulin-4 (1:10 molar ratio; identical conditions as tested for LTBP-4L). Fibulin-4 did not induce an extension of LTBP-4S (*SI Appendix*, Fig. S6 *A*, *Center*). Mixing tropoelastin with LTBP-4S and fibulin-4 did not result in multimerization of extended tropoelastin assemblies (*SI Appendix*, Fig. S6 *A*, *Right*). This suggests that the role of fibulin-4 in modifying the LTBP-4 structure and function and in promoting tropoelastin deposition is specific to LTBP-4L.

Discussion

Elastogenesis, the development of functional elastic fibers in blood vessels, lung, skin, and other tissues, is a hierarchical molecular process which involves a number of proteins with characteristic and distinct roles. The present study reveals molecular mechanisms in this process, emphasizing the significance of the interaction and interdependence between fibulin-4 and LTBP-4L, and the functional consequences on the central elastogenic proteins fibrillin-1, fibronectin, and tropoelastin. The study demonstrates a dual role of fibulin-4 in regard to LTBP-4L, 1) by inducing an extended conformation of LTBP-4L which alters self- and protein interaction properties, and 2) by escorting tropoelastin onto the extended and assembled LTBP-4L to allow linear deposition and assembly of elastic fibers. These results provide a mechanistic explanation of in vivo studies, which show the indispensable role of fibulin-4 in elastogenesis (1, 13, 31) and a functional link between LTBP-4L and fibulin-4 (24).

Most of the structural information in the fibrillin/LTBP superfamily stems from the analysis of fibrillin-1. Generally, tandem repeats of cbEGF domains in fibrillin-1 provide a relatively rigid extended conformation in their calcium-bound form and a more flexible conformation under calcium-free conditions (16–19). LTBP-4 contains the longest stretch of cbEGF domains (15) interspersed by 2 TB domains in the LTBP family, which should contribute up to 50 nm of length to the expected extended structure in its calcium-bound form (27–29). This provided the basis for various studies to assume LTBP-4 as an extended protein in their working models, which helped explain the linear assembly of tropoelastin onto microfibrils (11, 20). Here, we have recombinantly expressed LTBP-4L equipped with its endogenous signal peptide to allow proper posttranslational modification in the secretory pathway of human cells. Surprisingly, purified LTBP-4L primarily appeared as compact molecules in AFM analysis, but not as extended molecules. This correlates with a recent structural analysis of another member of the LTBP family, LTBP-1, that showed class averages shorter than expected with significant portions of compact molecules and termini folded inwards (32).

In a search for proteins that could modulate this compact LTBP-4L conformation, we identified fibulin-4, another elastogenic protein. Either in the presence of fibulin-4, or after transient exposure to fibulin-4, LTBP-4L changed its structure to the expected extended conformation with a length of ~80 nm. The compact conformation of LTBP-4L could potentially result from

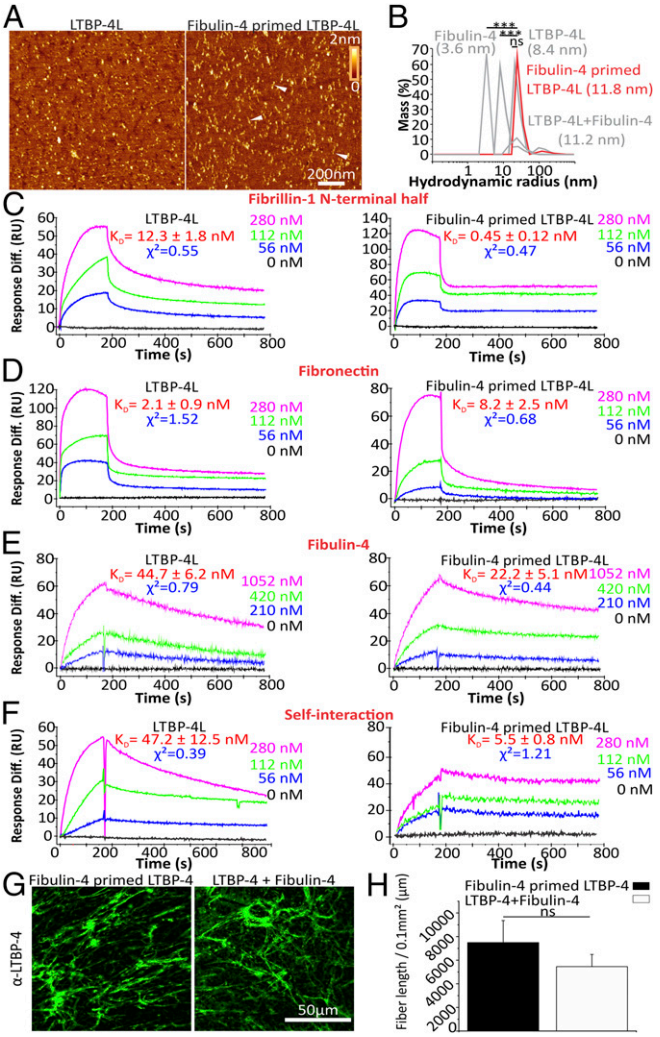

Fig. 6. A transient interaction with fibulin-4 is sufficient to induce conformational and functional change in LTBP-4L. (*A*) AFM height images showing LTBP-4L and fibulin-4 primed LTBP-4L. Arrowheads indicate some elongated molecules. (*B*) DLS mass distribution of fibulin-4–primed LTBP-4L (red curve) overlaid the profiles for fibulin-4, LTBP-4L, and of a 1:10 molar ratio LTBP-4L/fibulin-4 mixture from Fig. 3*C* (gray curves). Note the similarity in the hydrodynamic radius between fibulin-4–primed LTBP-4L and the LTBP-4L/fibulin-4 mixture, and the significant differences compared to fibulin-4 alone or LTBP-4L alone. The *x* axis shows the particle hydrodynamic radius on a logarithmic scale and the *y* axis the mass percentages of particles. ***$P < 0.0001$; ns indicates a nonsignificant *P* value (2-sample *t* test). (*C*–*F*) SPR sensorgrams of LTBP-4L (nonprimed; *Left*) or fibulin-4–primed LTBP-4L (*Right*) binding to fibrillin-1 N-terminal half (*C*), fibronectin (*D*), fibulin-4 (*E*), and to itself (LTBP-4L to LTBP-4L, and fibulin-4–primed LTBP-4L to fibulin-4–primed LTBP-4L) (*F*). Note the changes in binding affinities. (*G*) Comparison of LTBP-4L self-assembly by immunofluorescence between fibulin-4–primed LTBP-4L (10 µg/mL) and a mixture of LTBP-4L and fibulin-4 (10 µg/mL LTBP-4L and 27 µg/mL fibulin-4 equivalent to a 1:10 molar ratio) after addition to human skin fibroblasts. (*H*) Quantification of the total fiber length in *G*. Note that both conditions similarly promote LTBP-4L assembly.

self-interaction sites in LTBP-4L interacting within the same molecule, instead of with another one. We clearly demonstrate here that LTBP-4L contains high-affinity self-interaction properties. This correlates with recent data showing that LTBP-1 can self-interact (32). However, determining the precise location of self-interaction sites in LTBP-4 requires further mapping studies. Bultmann-Mellin et al. (25) showed that fibulin-4 interacts with the N terminus of both LTBP-4L and LTBP-4S, with a higher affinity for LTBP-4L, indicating that the N-terminal 4-Cys domains determine the higher affinity in LTBP-4L. We confirmed here the stronger binding of fibulin-4 to LTBP-4L compared to LTBP-4S. These differences in binding strength are likely the reason why fibulin-4 affects the structure and function of LTBP-4L but not of LTBP-4S. It is possible that the fibulin-4 and the self-interaction sites are topologically close together at the N terminus of LTBP-4L, resulting in fibulin-4 competing with intramolecular self-interaction, which would release the molecular clasp holding the molecule together in a compact form. Our real-time DLS data support this hypothesis. LTBP-4L oligomerizes upon fibulin-4 dissociation but reverts to the monomeric extended state upon reassociation with fibulin-4. This suggests that 1 of the self-interaction sites of LTBP-4L overlaps with the fibulin-4 binding region at the N terminus of LTBP-4L, and that fibulin-4 can compete with LTBP-4L oligomerization. This results in the 2 events being mutually exclusive, at least in vitro where fibrillin-1–containing microfibrils and fibronectin are not available to stabilize LTBP-4 oligomerization and assembly (4).

How can a tandem repeat of cbEGF domains adopt a compact conformation? We hypothesized that some of the calcium binding sites in cbEGFs domains may not be accessible for calcium in the compact form of LTBP-4L, allowing more flexibility and back-folding through intramolecular interactions. When fibulin-4 interacts with LTBP-4L it releases the molecular clasp and opens up the LTBP-4L structure, which in turn would make cbEGF domains available for calcium binding. This would change LTBP-4L from a flexible and compact molecule to a more rigid and extended molecule. This hypothesis was supported by calcium chelation experiments. When treated with EDTA, the extended LTBP-4L conformation, induced by fibulin-4, reverted to the compact conformation, confirming that calcium is essential for stabilization of the extended conformation. This also explains our data, which demonstrate that a transient LTBP-4L exposure with fibulin-4 is sufficient to induce a stable conformational and functional change in LTBP-4L, even after fibulin-4 has dissociated. Once, when the cbEGF domains are saturated with calcium, the molecule rigidifies as was described for tandem cbEGF repeats in fibrillin-1 (16–19). This would keep the self-interaction sites apart and make them available for the interaction with either other LTBP-4 molecules or with fibrillin-1. Overall, our results define the mechanism by which LTBP-4L, mediated by fibulin-4, attains an extended structure and explain the assumed conformation of LTBP-4L in various speculative elastogenic models (11, 20).

The propensity of fibulin-4 to multimerize is a key factor in the molecular mechanism of elastic fiber assembly and formation. We show that only fibulin-4 multimers interact with LTBP-4L, as well as with fibronectin, whereas these protein interactions were not detectable with monomeric fibulin-4. This explains why only fibulin-4 multimers have the capacity to transform LTBP-4L from a compact to an elongated conformation, but not the monomers. Fibulin-4 multimerization could increase the avidity for binding LTBP-4L and other proteins by clustering up to 10 molecules in a disk-shaped particle (15). Here, we have mapped the binding sites for LTBP-4L to 2 binding epitopes, 1 in the central and 1 in the C-terminal region of fibulin-4. How these binding sites are topologically situated within a multimeric unit remains to be established. Another possibility is that the LTPB-4L binding sites in fibulin-4 operate in a cooperative manner that requires conformational changes in subunits to increase the affinity for LTBP-4L. However, based on the structural constraints of disulfide bonds throughout the fibulin-4 molecule, we consider this possibility unlikely. These data extend the concept of multimerization generating additional functions in elastogenic proteins, which we had previously shown for fibrillin-1 (3, 33). Overall, the data show that fibulin-4 first requires self-interaction and multimerization before it can induce a conformational and functional change in LTBP-4L.

We have also tested the capability of fibulin-5 to guide structural and functional changes of LTBP-4L, because of its similarity to fibulin-4 and its importance in elastogenesis. Upon interaction with fibulin-5, LTBP-4L changed its structure to an extended

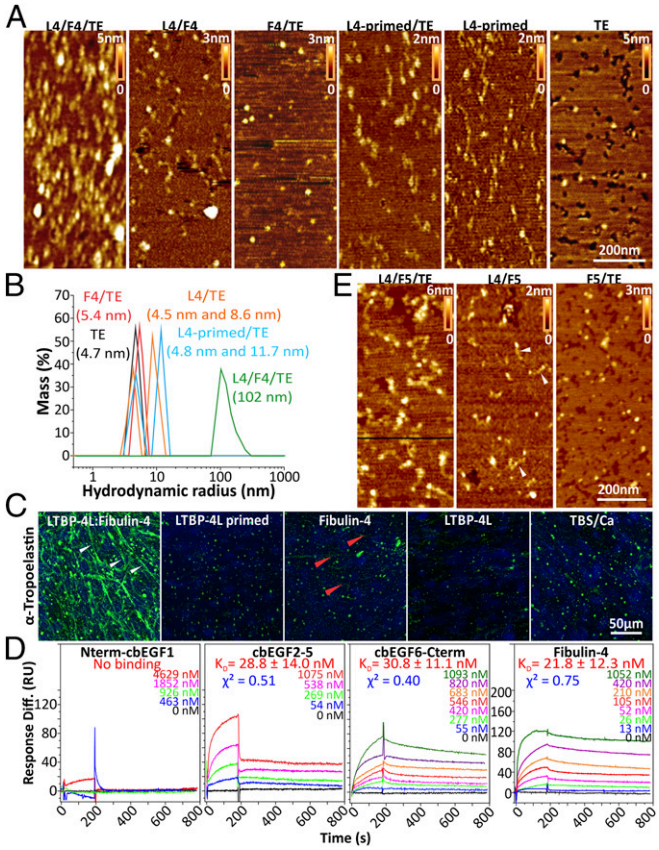

Fig. 7. Role of fibulin-4 and LTBP-4L in tropoelastin aggregation and binding. (*A*) AFM height images of tropoelastin (TE) together with either the LTBP-4L/fibulin-4 mixture (L4/F4/TE), the fibulin-4–primed LTBP-4L (L4-primed/TE), or fibulin-4 (F4/TE). As controls, the LTBP-4L/fibulin-4 mixture (L4/F4), the fibulin-4 primed LTBP-4L (L4-primed), or TE alone are shown. (*B*) DLS mass distribution of TE alone or mixed with either fibulin-4 (F4/TE), LTBP-4L (L4/TE), fibulin-4–primed LTBP-4L (L4-primed/TE) or the LTBP-4L/fibulin-4 mixture (L4/F4/TE). The *x* axis represents the particle hydrodynamic radius on a logarithmic scale, and the *y* axis the particle mass percentages. Note the shift in hydrodynamic radius to large size (*B*) and the large assembly structures formed (*A*) only in the presence of LTBP-4L, fibulin-4, and tropoelastin together. (*C*) Elastin assembly in the extracellular matrix of human skin fibroblasts supplemented with either a mixture of 10 μg/mL LTBP-4L and 27 μg/mL fibulin-4 (1:10 molar ratio), or 10 μg/mL fibulin-4 primed LTBP-4L, or 10 μg/mL LTBP-4L alone, or 27 μg/mL fibulin-4 alone. TBS/2 mM $CaCl_2$ was used as buffer control. (*D*) SPR binding assays with soluble Nterm-cbEGF1, cbEGF2-5, and cbEGF6-Cterm fibulin-4 fragments and immobilized tropoelastin. Note that the binding sites are located in the center and the C-terminal region of fibulin-4. (*E*) AFM height images of tropoelastin (TE) together with either a LTBP-4L/fibulin-5 mixture (L4/F5/TE) or fibulin-5 (F5/TE). As control, the LTBP-4L/fibulin-5 mixture (L4/F5) is shown.

conformation, albeit at a significant lower extent and efficiency. The structural changes were not sufficient to elicit the functional changes in terms of fibrillin-1 or fibronectin binding observed upon fibulin-4 interaction. In addition, tropoelastin deposition onto the extended LTBP-4L was less developed as compared to the fibulin-4–treated LTBP-4L. Such a mechanism would explain why fibulin-4 deficiency typically has more severe effects on elastic fibers compared to fibulin-5 deficiency (31, 34, 35).

Fibronectin has emerged as a master organizer required for the assembly of various extracellular matrix proteins, including fibrillin-1 (2, 3), fibulin-1 (36, 37), LTBP-1 (38), LTBP-4 (4, 5), collagen I and III (39–43), fibrinogen (44), thrombospondin-1 (40), and tenascin-C (45). The dependency of LTBP-4 assembly on fibronectin is mediated via fibrillin-1 (5). We recently showed through cell culture and mouse models that both the cellular and the plasma form of fibronectin are essential for the assembly/deposition of fibulin-4 in the aorta (6). Similar to LTBP-4, fibulin-4 also interacts with fibrillin-1 (26). Whether fibulin-4 assembly is directly dependent on fibronectin or is mediated via fibrillin-1 was not yet clear. Here, we present evidence demonstrating that fibrillin-1 is not required for the assembly of fibulin-4, but fibronectin is. These are critical aspects for the development of a model for the roles of fibulin-4 and LTBP-4 in elastic fiber formation (see below). However, whether or not other extracellular matrix proteins known to be dependent on fibronectin potentially play a role in fibulin-4 assembly requires further analysis.

Solid-phase binding assays have previously shown that LTBP-4S does not directly interact with tropoelastin but requires the presence of fibulin-5 as an adapter, suggesting that the promoting effect of LTBP-4S on tropoelastin deposition is dependent on fibulin-5 (11). Dabovic et al. (20) observed impaired elastogenesis in *Ltbp4S*$^{-/-}$ mice (deficiency of LTBP-4S), which improved in *Ltbp4S*$^{-/-}$*; Fbln5*$^{-/-}$ double-knockout mice (LTBP-4L and fibulin-4 present). These authors speculated a role of fibulin-4, in the absence of both LTBP-4S and fibulin-5, in improving elastogenesis. In another study, a reduced LTBP-4L interaction with fibulin-4 was speculated as the cause of severely compromised elastogenesis observed in *Ltbp4S*$^{-/-}$*; Fbln4*$^{R/R}$ mice (LTBP-4L present and fibulin-4 reduced to 25%) (24). Taken together, these data suggested a functional link between fibulin-5 and LTBP-4S, and fibulin-4 and LTBP-4L, in promoting elastogenesis. We provide further support for this concept by demonstrating that fibulin-4 cannot promote structural changes in LTBP-4S. But how the fibulins and LTBP-4 isoforms influenced each other and how they function together was not clear. Our data show the necessity for both fibulin-4 and the fibulin-4–induced extended LTBP-4L in the formation of large tropoelastin assemblies, which identifies the molecular mechanism explaining the in vivo observations and speculative models from the articles outlined above.

Based on the results presented here, and on the existing literature, we propose the following model for the roles of fibulin-4 and LTBP-4L in elastogenesis (Fig. 8). 1) Fibronectin fibers appear early in cell culture and during elastic tissue development (40), followed by fibrillin-1 expression and fibronectin-dependent assembly into microfibrils (2, 3, 6). 2) Later, fibulin-4 is secreted and forms multimers, whereas 3) LTBP-4L remains in a compact monomeric conformation directly after secretion. 4) Both deposit on a fibronectin network that localizes them in physical proximity. 5) Fibulin-4 multimers then compete with the intramolecular self-interaction of LTBP-4L (4, 25) to induce a calcium binding-driven conformational change in LTBP-4L from a compact to an extended shape. This extension exposes the fibrillin-1 binding site at the C-terminal region of LTBP-4L (5, 46). 6) The 2 proteins dissociate, facilitating self-assembly of the extended LTBP-4L, transfer onto fibrillin-1-containing microfibrils (4) and linear deposition (4, 11). Simultaneously, fibulin-4 interacts with tropoelastin (10, 12), and microfibrils separate from the fibronectin network (7). 7) Fibulin-4 deposits tropoelastin onto the linearly assembled LTBP-4L molecules, forming nascent elastic fibers.

In conclusion, our results highlight mechanisms associated with the elastogenic proteins fibulin-4, LTBP-4, fibronectin, fibrillin-1, and tropoelastin, which control elastic matrix assembly. The data provide a paradigm of how elastic fibers assemble.

Methods

Extended details for all methods are available in *SI Appendix, Materials and Methods*.

Protein Purification. Recombinant histidine-tagged full-length fibulin-4, fibulin-5, LTBP-4L, and LTBP-4S, as well as fibulin-4 fragments were generated in HEK293 cells and purified using procedures described previously (15). The LTBP-4 constructs contained the endogenous signal peptide, whereas all of the fibulin-4 fragments were designed with the BM40 signal peptide at the N terminus to ensure proper secretion, folding, and posttranslational modifications. The N-terminal half of fibrillin-1 and highly purified human

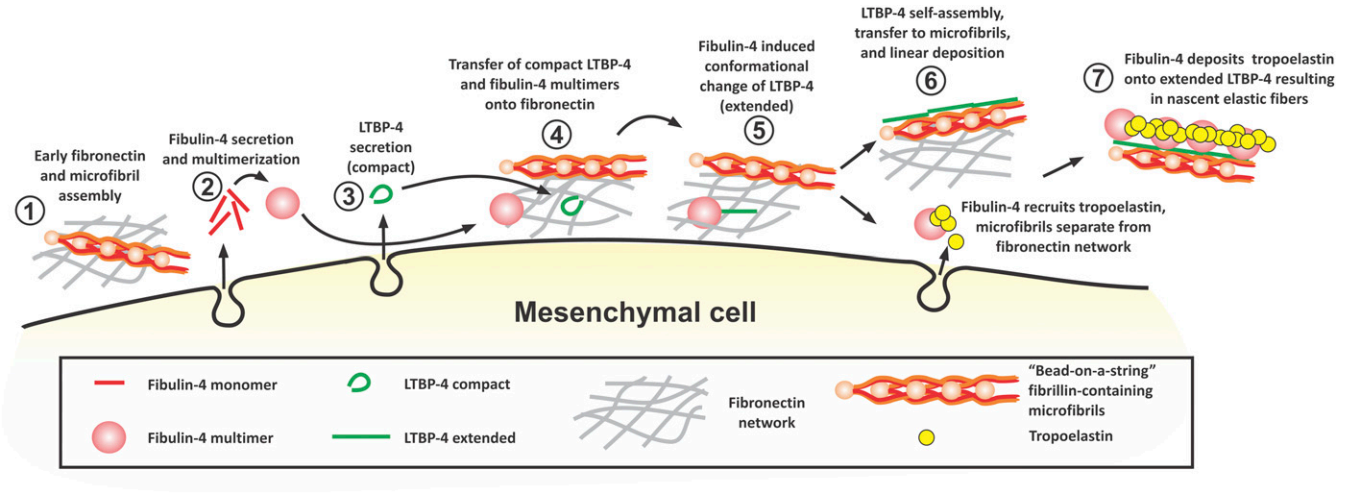

Fig. 8. Schematic representation of the proposed elastogenic model highlighting the role of fibulin-4 and LTBP-4L. Details are described in the text.

plasma fibronectin were produced as previously described (47, 48). Recombinant human tropoelastin was purchased (Elastagen).

DLS Measurements. DLS experiments were performed as previously published with minor modifications (49).

Protein Binding Assays. SPR spectroscopy was performed to study the binding characteristics and the kinetics of interaction of various proteins and protein fragments (Biacore X; GE Healthcare Life Sciences). The ligand was immobilized on CM5 and C1 sensor chips by standard amine coupling, resulting in immobilization of 200 to 1,000 resonance units. The second channel was used as a control. Kinetic analyses were performed at 0- to 200-μg/mL concentration of the analyte at a 10-μL/min flow rate for 180 s (association), and dissociation was monitored for 600 s. The affinity constants were evaluated from kinetics data (fitted rate constants) (BIAevaluation software 4.1; GE Healthcare Life Sciences), using the module "Fit Kinetics Separate ka/kd" with the 1:1 Langmuir binding model. The equilibrium dissociation constant (K_D) was calculated as the k_d/k_a ratio, averaged over all concentrations injected.

Solid-phase binding assays were employed to determine interactions of LTBP-4L in mixtures (LTBP-4L:fibulin-4 and LTBP-4L:fibulin-5) with either immobilized fibrillin-1 or fibronectin following a previously established protocol (15).

AFM. AFM experiments were performed as previously described (15). The analyses were conducted with either LTBP-4L alone or in a mixture (1:10 molar ratio) with fibulin-4 (nongel-filtrated, or gel-filtrated fibulin-4 monomers, dimers, or multimers), or primed with fibulin-4 alone, or with fibulin-5 (nongel-filtrated; 1:10 molar ratio). In addition, experiments were conducted with LTBP-4S alone or in a mixture with fibulin-4. Tropoelastin was added as indicated. Quantification of sizes, shapes, and abundances of particles was performed by postprocessing of AFM height images using the WSxM 5.0 Develop 1.1 software (50). Shape quantification was conducted by binning the molecules into 3 classes (i.e., compact, semicompact, and elongated). Molecular structures with more complex shapes or aggregates were excluded.

Cell Culture Experiments. To assess the consequences of the fibulin-4–induced LTBP-4L conformational change on the assembly of LTBP-4 or elastin, proteins were added to human skin fibroblasts at the time of cell seeding (Montreal Children's Hospital Research Ethics Board Approval PED-06-054). The cells were fixed after 7 d and analyzed by immunofluorescence, as described previously (3). Similarly, to assess the dependency of fibulin-4 assembly on fibrillin-1, wild-type (*Fbn1*$^{+/+}$) and *Fbn1*$^{-/-}$ mouse skin fibroblasts were cultured for 4 d followed by immunofluorescence. Mouse skin fibroblasts from *Fn*$^{+/+}$ and inducible *Fn*$^{-/-}$ (as described in ref. 6) were utilized to confirm the dependency of fibulin-4 assembly on fibronectin. Since both mouse primary cells produced very little fibulin-4 fibers, 25 μg/mL of purified fibulin-4 was added for 1 d before fixation and analysis by immunofluorescence.

Tissue Immunofluorescence. Paraffin sections of the aortae from embryonic day 17.5 wild-type and fibulin-4 knockout mice were stained using anti-mouse LTBP-4 antiserum (1:1,000).

Preparation and Analysis of Fibulin-4–Primed LTBP-4. Seven milligrams of purified fibulin-4 were coupled to 1 mL CNBr-activated Sepharose 4B according to the manufacturer's instructions (GE Healthcare). LTBP-4L (0.4-mg starting material) was passed over this column over an extended timespan of 200 min (at 15 μL/min) to allow binding and dissociation of LTBP-4. This procedure facilitated a transient interaction between the 2 proteins.

Statistics. Two-sample *t* test was used to determine the significance of the difference in the structural parameters of LTBP-4L, the protein hydrodynamic radii, the protein staining intensities (tissue immunofluorescence), and branch length (protein assemblies). For all statistical analyses, $^{*}P < 0.05$, $^{**}P < 0.01$, $^{***}P < 0.0001$, and $^{\dagger}P < 0.01$. Nonsignificance is labeled "ns."

ACKNOWLEDGMENTS. We thank Dr. Dirk Hubmacher, Dr. Suneel Apte, and Dr. Francesco Ramirez for kindly providing skin fibroblasts from *Fbn1*$^{-/-}$ mice; Dr. Deane F. Mosher for providing the highly purified human plasma fibronectin; Dr. Jean-Martin Laberge for help obtaining foreskin fibroblasts; and Chae Syng Lee, Kungjun Lee, and Aviva Zhao for constant support with protein production and purification.

1. C. L. Papke, H. Yanagisawa, Fibulin-4 and fibulin-5 in elastogenesis and beyond: Insights from mouse and human studies. *Matrix Biol.* **37**, 142–149 (2014).
2. R. Kinsey *et al.*, Fibrillin-1 microfibril deposition is dependent on fibronectin assembly. *J. Cell Sci.* **121**, 2696–2704 (2008).
3. L. Sabatier *et al.*, Fibrillin assembly requires fibronectin. *Mol. Biol. Cell* **20**, 846–858 (2009).
4. A. K. Kantola, J. Keski-Oja, K. Koli, Fibronectin and heparin binding domains of latent TGF-beta binding protein (LTBP)-4 mediate matrix targeting and cell adhesion. *Exp. Cell Res.* **314**, 2488–2500 (2008).
5. R. N. Ono *et al.*, Latent transforming growth factor beta-binding proteins and fibulins compete for fibrillin-1 and exhibit exquisite specificities in binding sites. *J. Biol. Chem.* **284**, 16872–16881 (2009).
6. H. Kumra *et al.*, Roles of fibronectin isoforms in neonatal vascular development and matrix integrity. *PLoS Biol.* **16**, e2004812 (2018).
7. L. Sabatier *et al.*, Complex contributions of fibronectin to initiation and maturation of microfibrils. *Biochem. J.* **456**, 283–295 (2013).
8. F. Sato *et al.*, Distinct steps of cross-linking, self-association, and maturation of tropoelastin are necessary for elastic fiber formation. *J. Mol. Biol.* **369**, 841–851 (2007).
9. B. A. Kozel *et al.*, Elastic fiber formation: A dynamic view of extracellular matrix assembly using timer reporters. *J. Cell. Physiol.* **207**, 87–96 (2006).
10. Y. Yamauchi, E. Tsuruga, K. Nakashima, Y. Sawa, H. Ishikawa, Fibulin-4 and -5, but not Fibulin-2, are associated with tropoelastin deposition in elastin-producing cell culture. *Acta Histochem. Cytochem.* **43**, 131–138 (2010).
11. K. Noda *et al.*, Latent TGF-β binding protein 4 promotes elastic fiber assembly by interacting with fibulin-5. *Proc. Natl. Acad. Sci. U.S.A.* **110**, 2852–2857 (2013).
12. R. Choudhury *et al.*, Differential regulation of elastic fiber formation by fibulin-4 and -5. *J. Biol. Chem.* **284**, 24553–24567 (2009).

13. M. Horiguchi *et al*., Fibulin-4 conducts proper elastogenesis via interaction with cross-linking enzyme lysyl oxidase. *Proc. Natl. Acad. Sci. U.S.A.* **106**, 19029–19034 (2009).
14. M. Hirai *et al*., Fibulin-5/DANCE has an elastogenic organizer activity that is abrogated by proteolytic cleavage in vivo. *J. Cell Biol.* **176**, 1061–1071 (2007).
15. J. Djokic, C. Fagotto-Kaufmann, R. Bartels, V. Nelea, D. P. Reinhardt, Fibulin-3, -4, and -5 are highly susceptible to proteolysis, interact with cells and heparin, and form multimers. *J. Biol. Chem.* **288**, 22821–22835 (2013).
16. D. P. Reinhardt *et al*., Calcium determines the shape of fibrillin. *J. Biol. Chem.* **272**, 7368–7373 (1997).
17. T. J. Wess *et al*., Calcium determines the supramolecular organization of fibrillin-rich microfibrils. *J. Cell Biol.* **141**, 829–837 (1998).
18. C. M. Kielty, C. A. Shuttleworth, The role of calcium in the organization of fibrillin microfibrils. *FEBS Lett.* **336**, 323–326 (1993).
19. A. K. Downing *et al*., Solution structure of a pair of calcium-binding epidermal growth factor-like domains: Implications for the Marfan syndrome and other genetic disorders. *Cell* **85**, 597–605 (1996).
20. B. Dabovic *et al*., Function of latent TGFβ binding protein 4 and fibulin 5 in elastogenesis and lung development. *J. Cell. Physiol.* **230**, 226–236 (2015).
21. J. Saharinen, J. Taipale, O. Monni, J. Keski-Oja, Identification and characterization of a new latent transforming growth factor-beta-binding protein, LTBP-4. *J. Biol. Chem.* **273**, 18459–18469 (1998).
22. A. K. Kantola, M. J. Ryynänen, F. Lhota, J. Keski-Oja, K. Koli, Independent regulation of short and long forms of latent TGF-beta binding protein (LTBP)-4 in cultured fibroblasts and human tissues. *J. Cell. Physiol.* **223**, 727–736 (2010).
23. B. A. Kozel, D. Hubmacher, "Pathology of the elastic matrix" in *Elastic Fiber Matrices—Biomimetic Approaches to Regeneration and Repair*, A. Ramamurthi, C. Kothapalli Eds., (CRC Press, Boca Raton, FL, ed. 1, 2016), pp. 31–80.
24. I. Bultmann-Mellin *et al*., Function of Ltbp-4L and fibulin-4 in survival and elastogenesis in mice. *Dis. Model. Mech.* **9**, 1367–1374 (2016).
25. I. Bultmann-Mellin *et al*., Modeling autosomal recessive cutis laxa type 1C in mice reveals distinct functions for Ltbp-4 isoforms. *Dis. Model. Mech.* **8**, 403–415 (2015).
26. E. El-Hallous *et al*., Fibrillin-1 interactions with fibulins depend on the first hybrid domain and provide an adaptor function to tropoelastin. *J. Biol. Chem.* **282**, 8935–8946 (2007).
27. D. P. Reinhardt *et al*., Fibrillin-1: Organization in microfibrils and structural properties. *J. Mol. Biol.* **258**, 104–116 (1996).
28. S. A. Jensen, S. Iqbal, E. D. Lowe, C. Redfield, P. A. Handford, Structure and interdomain interactions of a hybrid domain: A disulphide-rich module of the fibrillin/LTBP superfamily of matrix proteins. *Structure* **17**, 759–768 (2009).
29. S. S. Lee *et al*., Structure of the integrin binding fragment from fibrillin-1 gives new insights into microfibril organization. *Structure* **12**, 717–729 (2004).
30. J. Huang *et al*., Fibulin-4 deficiency results in ascending aortic aneurysms: A potential link between abnormal smooth muscle cell phenotype and aneurysm progression. *Circ. Res.* **106**, 583–592 (2010).
31. P. J. McLaughlin *et al*., Targeted disruption of fibulin-4 abolishes elastogenesis and causes perinatal lethality in mice. *Mol. Cell. Biol.* **26**, 1700–1709 (2006).
32. H. Troilo, R. Steer, R. F. Collins, C. M. Kielty, C. Baldock, Independent multimerization of Latent TGFβ Binding Protein-1 stabilized by cross-linking and enhanced by heparan sulfate. *Sci. Rep.* **6**, 34347 (2016).
33. D. Hubmacher *et al*., Biogenesis of extracellular microfibrils: Multimerization of the fibrillin-1 C terminus into bead-like structures enables self-assembly. *Proc. Natl. Acad. Sci. U.S.A.* **105**, 6548–6553 (2008).
34. T. Nakamura *et al*., Fibulin-5/DANCE is essential for elastogenesis in vivo. *Nature* **415**, 171–175 (2002).
35. H. Yanagisawa *et al*., Fibulin-5 is an elastin-binding protein essential for elastic fibre development in vivo. *Nature* **415**, 168–171 (2002).
36. S. Godyna, D. M. Mann, W. S. Argraves, A quantitative analysis of the incorporation of fibulin-1 into extracellular matrix indicates that fibronectin assembly is required. *Matrix Biol.* **14**, 467–477 (1995).
37. J. Roman, J. A. McDonald, Fibulin's organization into the extracellular matrix of fetal lung fibroblasts is dependent on fibronectin matrix assembly. *Am. J. Respir. Cell Mol. Biol.* **8**, 538–545 (1993).
38. S. L. Dallas *et al*., Fibronectin regulates latent transforming growth factor-beta (TGF beta) by controlling matrix assembly of latent TGF beta-binding protein-1. *J. Biol. Chem.* **280**, 18871–18880 (2005).
39. J. A. McDonald, D. G. Kelley, T. J. Broekelmann, Role of fibronectin in collagen deposition: Fab' to the gelatin-binding domain of fibronectin inhibits both fibronectin and collagen organization in fibroblast extracellular matrix. *J. Cell Biol.* **92**, 485–492 (1982).
40. J. Sottile, D. C. Hocking, Fibronectin polymerization regulates the composition and stability of extracellular matrix fibrils and cell-matrix adhesions. *Mol. Biol. Cell* **13**, 3546–3559 (2002).
41. T. Velling, J. Risteli, K. Wennerberg, D. F. Mosher, S. Johansson, Polymerization of type I and III collagens is dependent on fibronectin and enhanced by integrins alpha 11beta 1 and alpha 2beta 1. *J. Biol. Chem.* **277**, 37377–37381 (2002).
42. S. Li, C. Van Den Diepstraten, S. J. D'Souza, B. M. Chan, J. G. Pickering, Vascular smooth muscle cells orchestrate the assembly of type I collagen via alpha2beta1 integrin, RhoA, and fibronectin polymerization. *Am. J. Pathol.* **163**, 1045–1056 (2003).
43. K. E. Kadler, A. Hill, E. G. Canty-Laird, Collagen fibrillogenesis: Fibronectin, integrins, and minor collagens as organizers and nucleators. *Curr. Opin. Cell Biol.* **20**, 495–501 (2008).
44. M. Pereira *et al*., The incorporation of fibrinogen into extracellular matrix is dependent on active assembly of a fibronectin matrix. *J. Cell Sci.* **115**, 609–617 (2002).
45. C. Y. Chung, H. P. Erickson, Glycosaminoglycans modulate fibronectin matrix assembly and are essential for matrix incorporation of tenascin-C. *J. Cell Sci.* **110**, 1413–1419 (1997).
46. Z. Isogai *et al*., Latent transforming growth factor beta-binding protein 1 interacts with fibrillin and is a microfibril-associated protein. *J. Biol. Chem.* **278**, 2750–2757 (2003).
47. G. Lin *et al*., Homo- and heterotypic fibrillin-1 and -2 interactions constitute the basis for the assembly of microfibrils. *J. Biol. Chem.* **277**, 50795–50804 (2002).
48. D. F. Mosher, P. E. Schad, Cross-linking of fibronectin to collagen by blood coagulation Factor XIIIa. *J. Clin. Invest.* **64**, 781–787 (1979).
49. V. Nelea, Y. Nakano, M. T. Kaartinen, Size distribution and molecular associations of plasma fibronectin and fibronectin crosslinked by transglutaminase 2. *Protein J.* **27**, 223–233 (2008).
50. I. Horcas *et al*., WSXM: A software for scanning probe microscopy and a tool for nanotechnology. *Rev. Sci. Instrum.* **78**, 013705 (2007).